Int. J. Heat Mass Transfer. Vol. 12, pp. 595–609. Pergamon Press 1969. Printed in Great Britain

EVAPORATION AND COMBUSTION OF A FUEL DROPLET

S. KOTAKE and T. OKAZAKI

Institute of Space and Aeronautical Science, University of Tokyo, Meguro, Tokyo, Japan

(*Received* 27 *September* 1968)

Abstract—The process of evaporation and combustion of a liquid droplet in a still air is calculated numerically, treated as an unsteady diffusion-controlling phenomenon with the flame front model. Single droplets of liquid fuel—benzene, methyl alcohol, ethyl alcohol, *n*-octane—are evaporated and burned in air under various ambient temperatures, pressures and oxygen-concentrations. The process of evaporation can not attain to a quasi-steady state of mass and heat transfer at the droplet surface. Concerning combustion, the process approaches at its end to a quasi-steady state, though the values of the flame temperature and the ratio of the flame radius to the drop radius are much smaller than those of the quasi-steady theory. The initial condition of the surrounding air has a great influence on the process of evaporation and combustion.

NOMENCLATURE

- a, radius of flame front;
- b, radius of droplet;
- c_p, specific heat at constant pressure;
- D, diffusion coefficient;
- h, enthalpy per unit mass;
- h_c, heat of combustion per unit mass of fuel;
- h_l, latent heat of vaporization per unit mass of fuel;
- p, pressure;
- r, radial distance from center of droplet;
- R, gas constant;
- t, time;
- T, temperature;
- v, velocity;
- x, non-dimensional coordinates of r;
- Y, weight concentration.

Greek symbols

- α, thermal diffusivity;
- γ, stoichiometric oxygen-fuel mass ratio;
- λ, thermal conductivity;
- ρ, density.

Subscripts

- a, flame front;
- b, droplet surface;
- e, completion of evaporation or combustion;
- l, liquid;
- ∞, at infinite;
- 1, outside flame front;
- 2, between flame front and droplet surface (for combustion) or outside droplet (for evaporation);
- 3, inside droplet.

1. INTRODUCTION

THE PROBLEM for the combustion of fuel sprays has attracted the efforts of a number of researchers to study the physical and chemical processes involved in droplet combustion. Because of the complexity of the process, most of them have approached the problem by examining the evaporation and combustion of single droplets of fuel as a first step in understanding the overall phenomena.

Concerning the evaporation of a liquid droplet, a number of studies have been reported, especially in the meteorological field. Kobayashi [1] conducted numerical calculations of the evaporation of single droplets in air at high

temperatures with the assumption of constant Nusselt number on the droplet surface and showed the results in good agreement with his experimental ones.

Concerning the combustion of fuel droplets, Godsave [2] examined the burning droplet suspended on a fine quartz fiber and obtained a successful interpretation of his results on the assumption that the chemical reaction rates do not control the rate of burning, which succeeded in the considerable simplification of the analytical treatment for the combustion of fuel droplets. Spalding [3], also, showed with detailed experiments that one of the most controlling factor for the process should be the transfer or diffusion of mass and energy of the fuel vapor. Following these experimental results, Goldsmith and Penner [4] and Wise, Lorell and Wood [5] postulated a quasi-steady combustion model to develop the theoretical study of the burning process of fuel droplets. At the almost same time, Okazaki and Gomi [6] carried out independently a theoretical analysis similar to these. The mechanism of the combustion process of a fuel droplet postulated in common by these investigaters is as follows; the oxidizer delivered from the surrounding atmosphere and the fuel vapor evaporated from the droplet are diffused towards the flame front and consumed instantaneously upon reaching the flame front, of which location is defined by the condition that the ratio of the mass rate of delivery of fuel to oxygen at the point should be stoichiometric.

According to these theories of quasi-steady model, the burning rate (the mass flow rate of fuel vapor into the flame front) is proportional to the droplet radius. The flame is always located at the same position relative to the droplet surface. The temperature at the flame front is always constant. Experimental measurements of the burning rate reported by Kobayashi [7], Goldsmith [8], and Masdin and Thring [9] show that the relation of the proportionality of the mass burning rate to the droplet radius can be valid in a wide range of experimental conditions of burning droplets of the diameter of about 1 mm in the normal gravitational field, though they have appreciable discrepancies between calculated higher and observed lower values of the flame radius and the flame temperature. These satisfactory agreements between analytical and experimental values of the burning rate are accounted for by the fact that the changes in the flame temperature and in the flame radius would largely compensate for each other in the calculation of the burning rate.

The fuel droplets encountered in the spray combustions of actual engines are, however, of the diameter smaller by one order than those used in the experimental works, that is, of Grashof number smaller by three order. Upon the combustion of such a droplet, the gravity has less influence, so that the combustion process of the droplet must be investigated without any influence of natural convection, or in a near zero gravity field. Isoda and Kumagai [10] studied experimentally the combustion of fuel droplets in a near zero gravity field using a freely falling method, and showed that the transfers of heat and mass outside the flame should be not of quasi-steady state but of an unsteady phenomenon, so that the location of the flame front could not be predicted by the aforementioned theory of quasi-steady model. They made an attempt to treat the process with a transient diffusion-model in an approximate way, and obtained the calculated results in good agreement with their observed ones.

In the present study, we treat the evaporation and combustion of single droplets of fuel in a quiescent air as a more generally unsteady diffusion-controlling phenomenon with flame front model and calculate numerically the process with a digital computer.

2. EVAPORATION AND COMBUSTION OF A DROPLET

Following the theory of quasi-steady model for the evaporation and combustion of a droplet, we postulate the following assumptions for the mathematical description of the unsteady

model of the process; (i) the rate of the reaction of fuel-oxidation at the flame front is so fast compared to the delivery of combustible gases that the process should be controlled only by the transfer rate of mass and energy, (ii) the fuel vapor and the oxygen are delivered to the flame front at the rate of stoichiometric proportion and there consumed instantaneously to make the release of the entire heat of combustion, (iii) all conditions of the system are spherically symmetric, (iv) the effect of radiation is neglected.

First, we consider the governing equations of weight concentration, temperature and velocity of the mixture surrounding the droplet under these assumptions.

The mass transfers of fuel vapor and oxygen are mainly controlled by the convection of the mixture and by the molecular diffusion due to the difference of weight concentration, the diffusion due to the difference of pressure or temperature being neglected. Denoting the weight concentration of species Y, we can represent the relation of mass conservation in a spherically symmetrical system as

$$\frac{\partial \rho Y}{\partial t} + \frac{1}{r^2}\frac{\partial}{\partial r} r^2[\rho Y(v + v_Y)] = 0, \tag{1}$$

where r is the distance from the center of droplet, ρ the density of the mixture, v its velocity, and v_Y the diffusion velocity of the species under consideration, which is given for a binary mixture by

$$v_Y = -\frac{D}{Y}\frac{\partial Y}{\partial r}, \tag{2}$$

where D is the diffusion coefficient. Summing up equations (1) for all species, we obtain the equation of continuity for the mixture,

$$\frac{\partial \rho}{\partial t} + \frac{1}{r^2}\frac{\partial}{\partial r}(r^2 \rho v) = 0. \tag{3}$$

The relation of energy conservation in the same system without any production of energy can be written as

$$\frac{\partial \rho h}{\partial t} + \frac{1}{r^2}\frac{\partial}{\partial r} r^2[\rho h(v + v_h)] = 0, \tag{4}$$

where h is the enthalpy per unit mass of the mixture and v_h is the diffusion velocity of energy due to the heat conduction which is given by

$$v_h = -\frac{\lambda}{\rho h}\frac{\partial T}{\partial r}. \tag{5}$$

The equation of motion for an inviscid fluid is

$$\frac{\partial \rho v}{\partial t} + \frac{1}{r^2}\frac{\partial}{\partial r}(r^2 \rho v^2) = -\frac{\partial p}{\partial r}, \tag{6}$$

where p is the pressure, and the relation of the state of the mixture assumed as an ideal gas is

$$p = \rho R T. \tag{7}$$

At a spherical surface (r^*) of infinitesmal thickness, the continuity relations of these equations are expressed as

$$[\rho Y(v - \dot{r}^* + v_Y)]_+ = [\rho Y(v - \dot{r}^* + v_Y)]_- \tag{8}$$

$$[\rho(v - \dot{r}^*)]_+ = [\rho(v - \dot{r}^*)]_- \tag{9}$$

$$[\rho h(v - \dot{r}^* + v_h)]_+ = [\rho h(v - \dot{r}^* + v_h)]_- \tag{10}$$

$$[\rho v(v - \dot{r}^*) + p]_+ = [\rho v(v - \dot{r}^*) + p]_-, \tag{11}$$

where $\dot{r}^* = dr^*/dt$, and the subscripts + and − identify the quantities outside and inside the surface, respectively.

Introducing the non-dimensionalized quantities of $t, r, v, \rho, p, T, h, D, \lambda, c_p$, and R referred to the values (identified by subscript r) which have the following relations,

$$\frac{t_r v_r}{r_r} = 1 \quad \frac{\alpha_r}{v_r r_r} = 1 \quad D_r = \alpha_r$$

$$\lambda_r = \rho_r c_{pr} \alpha_r \quad h_r = c_{pr} T_r \quad p_r = \rho_r R_r T_r,$$

we can express the governing equations in the same form as equations (1) to (11) with an exception of replacing p with $p/M (M = \rho_r v_r^2/p_r)$.

Substituting equation (3) into equations (1) and (4) with the non-dimensionalized quantities yields

$$\frac{\partial Y}{\partial t} + v\frac{\partial Y}{\partial r} + \frac{1}{\rho r^2}\frac{\partial}{\partial r}(r^2 w_Y) = 0 \tag{12}$$

$$\frac{\partial h}{\partial t} + v\frac{\partial h}{\partial r} + \frac{1}{\rho r^2}\frac{\partial}{\partial r}(r^2 w_h) = 0, \qquad (13)$$

where

$$w_Y = -\rho D\frac{\partial Y}{\partial r}, \qquad w_h = -\lambda\frac{\partial T}{\partial r}.$$

If the specific heat at constant pressure c_p has little change in the domain of space under consideration, equation (13) is rewritten as

$$\frac{\partial T}{\partial t} + v\frac{\partial T}{\partial r} + \frac{1}{\rho r^2}\frac{\partial}{\partial r}(r^2 w_T) = 0, \qquad (14)$$

where

$$w_T = -\rho\alpha\frac{\partial T}{\partial r}.$$

Expressing the quantities concerning the diffusivities of mass and heat as

$$N_Y = \rho D, \quad N_T = \rho\alpha, \qquad (15)$$

from equations (12) and (14) we obtain the equations of concentration and temperature in a similar form as

$$\frac{\partial Y}{\partial t} + v\frac{\partial Y}{\partial t} - \frac{1}{\rho r^2}\frac{\partial}{\partial r}\left(r^2 N_Y\frac{\partial Y}{\partial r}\right) = 0 \qquad (16)$$

$$\frac{\partial T}{\partial t} + v\frac{\partial T}{\partial r} - \frac{1}{\rho r^2}\frac{\partial}{\partial r}\left(r^2 N_T\frac{\partial T}{\partial r}\right) = 0. \qquad (17)$$

These diffusivities of mass and heat of various fuel-vapors and air at one atmosphere, N_Y and N_T, which are used in the present numerical computations, are shown in Fig. 2. It is noted from the figure that these properties could be approximated by a linear function of temperature in a wide range of it.

The continuity relation of energy at a boundary surface, equation (10), is rewritten with equation (9) as

$$\rho_-(v_- - \dot{r}^*)(h_+ - h_-) = (w_h)_- - (w_h)_+.$$

This leads for a evaporating surface of liquid with the latent heat of vaporization h_l

$$\rho_- h_l(v_- - \dot{r}^*) = (w_h)_- - (w_h)_+. \qquad (18)$$

At a flame front, because of the heat release of reaction, equations of species (8) and of energy (10) are no longer valid. Instead of them, the aforementioned assumption (ii) of the stoichiometric proportion of the oxygen and fuel flows and the instantaneous heat release at the flame front yields the following relations,

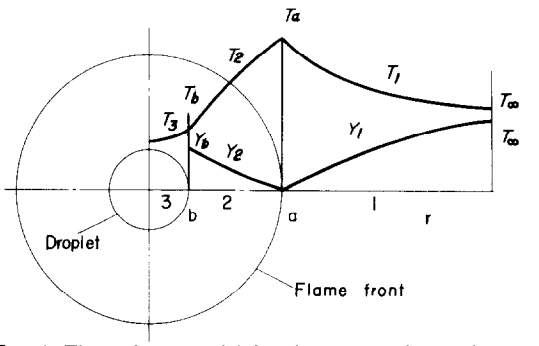

FIG. 1. Flame front model for the evaporation and combustion of a droplet.

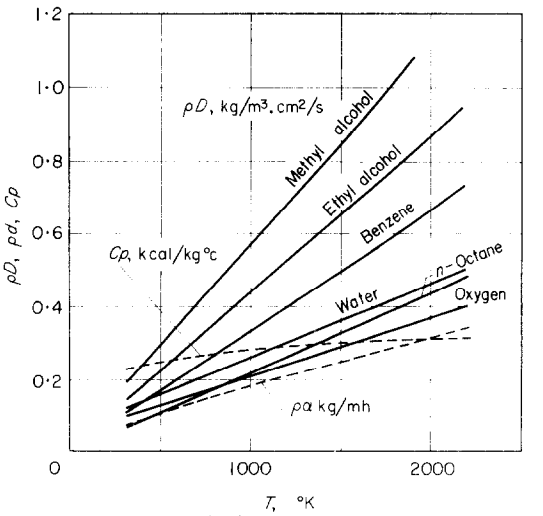

FIG. 2. Physical properties.

$$(w_Y)_+ = \gamma(w_Y)_- \qquad (19)$$

$$h_c(w_Y)_- = (w_h)_+ - (w_h)_-, \qquad (20)$$

where the subscripts + and − identify oxygen and fuel vapor, respectively, γ the stoichiometric mass ratio of oxygen to fuel vapor, and h_c the heat of combustion per unit mass of fuel vapor.

2.1 *Evaporation of a droplet*

First we treat the process of the evaporation of a droplet in a quiescent air. We identify the quantities outside the droplet by subscript 2

and the quantities inside the droplet by subscript 3 (Fig. 1) and use normalized coordinates (x) referred to the evaporating surface b defined by

$$r = bx \qquad (b \geqslant r \geqslant 0)$$
$$rx = b \qquad (r \geqslant b).$$

For the outside of droplet, the governing equations are given by equations (16), (17), (3) and (6) as follows:

$$\frac{\partial Y_2}{\partial t} - \frac{x^2}{b}\left[\left(v_2 - \frac{1}{x}\frac{db}{dt}\right)\frac{\partial Y_2}{\partial x} + \frac{x^2}{\rho_2}\frac{\partial}{\partial x}\left(\frac{w_{Y,2}}{x_2}\right)\right] = 0. \quad (21)$$

$$\frac{\partial T_2}{\partial t} - \frac{x^2}{b}\left[\left(v_2 - \frac{1}{x}\frac{db}{dt}\right)\frac{\partial T_2}{\partial x} + \frac{x^2}{\rho^2}\frac{\partial}{\partial x}\left(\frac{w_{T,2}}{x^2}\right)\right] = 0. \quad (22)$$

$$\frac{\partial \rho_2}{\partial t} + \frac{x}{b}\frac{db}{dt}\frac{\partial \rho_2}{\partial x} - \frac{x^2}{b}\left[x^2\frac{\partial}{\partial x}\left(\frac{\rho_2 v_2}{x^2}\right)\right] = 0. \quad (23)$$

$$\frac{\partial v_2}{\partial t} - \frac{x^2}{b}\left[\left(v_2 - \frac{1}{x}\frac{db}{dt}\right)\frac{\partial v_2}{\partial x} + \frac{1}{M\rho_2}\frac{\partial p_2}{\partial x}\right] = 0 \quad (24)$$

$$w_{Y,2} = N_{Y,2}\frac{x^2}{b}\frac{\partial Y_2}{\partial x}, \qquad w_{T,2} = N_{T,2}\frac{x^2}{b}\frac{\partial T_2}{\partial x},$$

where Y_2 is the weight concentration of fuel vapor.

For the inside of droplet, neglecting the motion of liquid and the change of the density of liquid, we have only the equation of temperature

$$\frac{\partial T_3}{\partial t} - \frac{x}{b}\frac{db}{dt}\frac{\partial T_3}{\partial x} - \frac{1}{\rho_3}\frac{1}{bx^2}\frac{\partial}{\partial x}(x^2 w_{T,3}) = 0, \quad (25)$$

where

$$w_{T,3} = -N_{T,3}\frac{1}{b}\frac{\partial T_3}{\partial x}.$$

The boundary conditions at a large distance from the droplet surface are

$$T_2 = T_\infty, \qquad p_2 = p_\infty, \qquad Y_2 = Y_\infty. \quad (26)$$

The boundary conditions at the droplet surface, equations (8), (9), and (18), are rewritten as

$$\frac{db^2}{dt} = -\frac{2}{\rho_3}\left[\frac{N_{Y,2}}{1 - Y_2}\frac{\partial Y_2}{dx}\right]_{x=1} \quad (27)$$

$$(v_2)_{x=1} = \left(1 - \frac{\rho_3}{\rho_2}\right)_{x=1}\frac{db}{dt} \quad (28)$$

$$\frac{h_l\rho_3}{2}\frac{db^2}{dt} = \left[\lambda_2\frac{\partial T_2}{\partial x} + \lambda_3\frac{\partial T_3}{\partial x}\right]_{x=1} \quad (29)$$

In addition to them, the condition of spherical symmetry leads the following equation at the center of droplet,

$$\left(\frac{\partial T_3}{\partial x}\right)_{x=0} = 0. \quad (30)$$

The number of the boundary conditions including the equation of state of the mixture is four, while the quantities required to be determined at the droplet surface are T_2, Y_2, ρ_2, p_2, v_2, T_3, and b, seven in number. The equations (21) to (24) subjected to the boundary condition (26) restrict one quantity at the droplet surface. Consequently, two additional boundary conditions are necessary to complete the mathematical description of the evaporation of a droplet. For this reason, we take the following reasonable assumptions. (v) The temperature is continuous at the evaporating surface, that is,

$$(T_2)_{x=1} = (T_3)_{x=1}. \quad (31)$$

(vi) The vapor on the droplet surface is kept at saturation pressure corresponding to the surface temperature. Using the Clausius–Clapeyron relation

$$h_l = \frac{T}{\rho_v}\frac{dp'}{dT},$$

where ρ_v is the density of vapor and p' is the saturation pressure at T, we obtain from the assumption (vi)

$$(Y_2)_{x=1} = \exp\left[-\frac{h_l}{R_v T_s}\left(\frac{T_s}{T_2} - 1\right)_{x=1}\right], \quad (32)$$

where h_l is the latent heat of vaporization,

R_v the gas constant of vapor, T_s the boiling point of liquid.

For the initial conditions of the evaporation, we suppose a droplet of temperature T_l surrounded by a quiescent air at temperature T_∞ and pressure p_∞, that is,

$$T_2 = T_\infty (x \neq 1), \quad T_3 = (T_2)_{x=1} = T_l,$$
$$Y_2 = Y_\infty, \quad p_2 = p_\infty, \quad v_2 = 0, \quad b = 1. \tag{33}$$

Writing equations (21–33) in finite difference form with respect to space and time, we can calculate numerically the quantities by stepwise Δt in time starting from the initial condition (33). Figures 3 to 7 show the results of the numerical

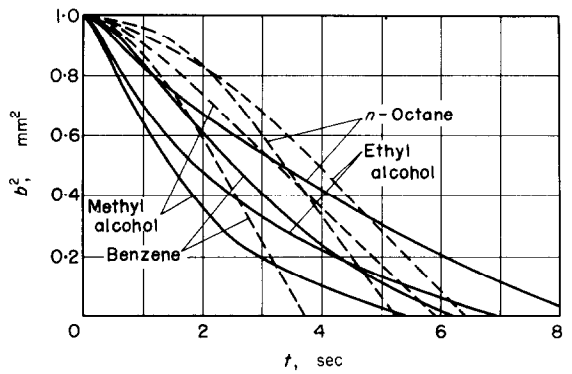

FIG. 3(a). Evaporation of a droplet (effect of fuel, T_∞ = 300°C).

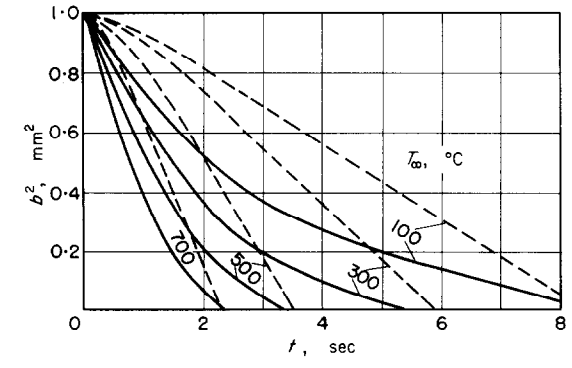

FIG. 3(b). Evaporation of a droplet (effect of ambient temperature, methyl alcohol).

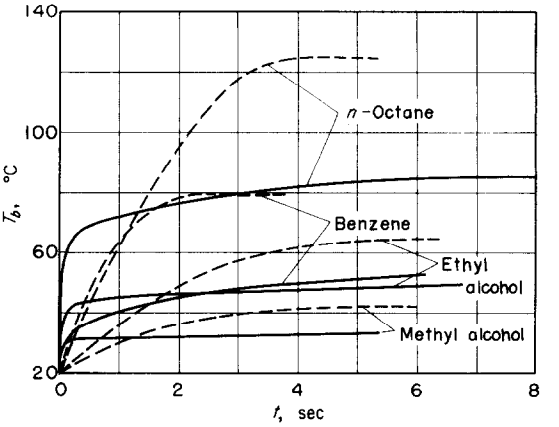

FIG. 4. Surface temperatures of evaporating droplets (T_∞ = 300°C).

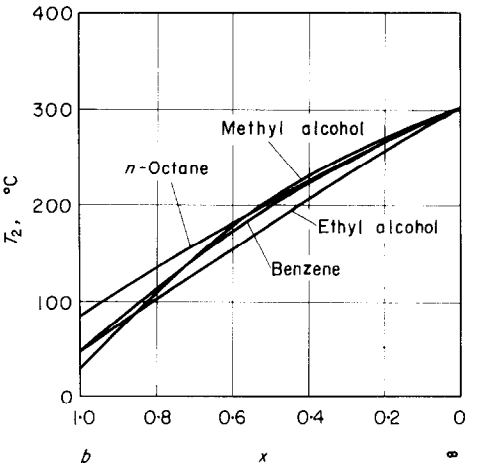

FIG. 5. Temperature distributions for evaporation (b = 0·5 mm, T_∞ = 300°C).

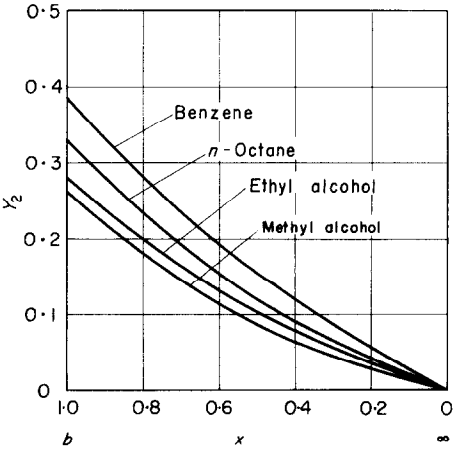

FIG. 6. Distribution of fuel-vapor concentration for evaporation (b = 0·5 mm, T_∞ = 300°C).

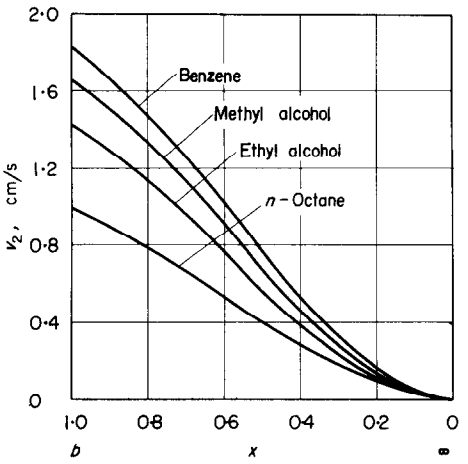

FIG. 7. Velocity distributions for evaporation (b = 0·5 mm, T = 300°C).

calculations of the evaporation of single droplets of benzene, methyl alcohol, ethyl alcohol, *n*-octane of the initial radius of 1 mm and the initial temperature of 20°C in a still hot air at atmospheric pressure under no existence of the fuel vapor. In these calculations, we used the physical properties of the liquids, their vapors, and air shown in Table 1 and Fig. 2. The meshes of space and time are $\Delta x = 0{\cdot}02$ and $\Delta t =$ (0·001–0·002) te, respectively, where te is the droplet life for evaporation.

Figure 3 shows the history of the evaporation of a droplet, that is, the relation of the droplet radius versus time; for various fuels at T_∞ = 300°C in Fig. 3(a) and at various temperatures for methyl alcohol in Fig. 3(b). The dotted lines in the figures represent the results obtained by solving the temperature field inside droplet with the assumption of constant transfer coefficients of mass (Sherwood number, Sh) and heat (Nusselt number, Nu) at the droplet surface, that is,

$$\left(\lambda_2 \frac{\partial T_2}{\partial x}\right)_{x=1} = Nu\lambda_2(T_\infty - T_2)_{x=1},$$

$$\left(D_2 \frac{\partial Y_2}{\partial x}\right)_{x=1} = Sh D_2(Y_\infty - Y_2)_{x=1}, \quad (34)$$

where $Nu = Sh = 1$ are assumed as in the study of Kobayashi [1]. It is noted from these figures that the features of evaporation, especially of methyl alcohol and ethyl alcohol, should be appreciably different from those obtained with the assumption (34). The evaporation curves in dotted lines are convex, while those of unsteady model are concave, being resulted from the fact that the dotted curves assume the process of evaporation in quasi-steady state contrary to the unsteady evaporation for the solid curves. Since $|db^2/dt| \propto Y_b/(1 - Y_b)$ according to equation (34), the evaporation curves are always convex under such a condition as long as Y_b is an increasing function of time. On the contrary, equation (27) with little change in Y_b (Fig. 4) shows $|db^2/dt| \propto |\partial Y_2/\partial x|_{x=1}$ in which $|\partial Y_2/\partial x|_{x=1}$ is a decreasing

Table 1

	Benzene	Methyl alcohol	Ethyl alcohol	*n*-Octane
ρ_l (Kg/m^3)	874	765	790	635
$c_{p,l}$ (Kcal/Kg°C)	0·44	0·62	0·58	0·60
λ_l (Kcal/mh°C)	0·100	0·170	0·157	0·135
α_l (m^2/h)	0·260	0·360	0·344	0·355
T_s (°C)	80	65	78	126
h_l (Kcal/Kg)	94	265	204	71
h_c (Kcal/Kg)	9620	4600	6460	10600
γ	3·08	1·50	2·09	3·51
R (m/°K)	10·85	26·50	18·43	7·43
D_0* (cm^2/s)	0·077	0·133	0·102	0·051

* In air $D = D_0(T/273)^{2\cdot0}\,1/P$ (T: °K, P: atm.).

function of time, so that the evaporation curves become concave. The discrepancies between these evaporation curves are more emphasized for the cases of methyl alcohol and ethyl alcohol, which have larger values of the diffusion coefficients of mass and heat.

Figure 4 shows the temperature at the surface of an evaporating droplet, the dotted curves being also obtained with the assumption (34). The surface temperature increases rapidly at the beginning of evaporation and then approaches gradually a value lower than the boiling point of the liquid. The asymptotic value of the surface temperature is so more close to the boiling point as the liquid is of a smaller value of the latent heat of vaporization, and is considerably higher in the case of quasi-steady model than in the unsteady model. In the latter, the amounts of mass and heat convected by the flow of evaporated vapor are taken into account. It would therefore be appreciated that the convections of mass and heat by the evaporated vapor flow have a considerable effect upon the process of evaporation.

Figures 5–7 are the distributions of the temperature T_2, the weight concentration of fuel vapor Y_2 and the velocity of the mixture of air and fuel vapor v_2, respectively, at the time when the droplet radius becomes a half of the initial value.

2.2 *Combustion of a droplet*

Letting the locations of the flame front and the droplet surface be $r = a$ and $r = b$, respectively, and denoting the quantities outside the flame front by subscript 1, between the flame front and the droplet surface by subscript 2 and inside the droplet by subscript 3 (Fig. 1), from equations (16), (17), (3), (6) and (7) with the use of a normalized coordinates (x) defined by

$$r = bx \qquad (b \geqslant r \geqslant 0)$$

$$r = (a - b)\quad x + b \qquad (a \geqslant r \geqslant b)$$

$$rx = a \qquad (r \geqslant a),$$

we obtain the governing equations for the combustion of a droplet as follows;

$$\frac{\partial Y_1}{\partial t} - \frac{x^2}{a}\left[\left(v_1 - \frac{1}{x}\frac{\mathrm{d}a}{\mathrm{d}t}\right)\frac{\partial Y_1}{\partial x} + \frac{x^2}{\rho_1}\frac{\partial}{\partial x}\left(\frac{w_{Y,1}}{x^2}\right)\right] = 0 \tag{35}$$

$$\frac{\partial T_1}{\partial t} - \frac{x^2}{a}\left[\left(v_1 - \frac{1}{x}\frac{\mathrm{d}a}{\mathrm{d}t}\right)\frac{\partial T_1}{\partial x} + \frac{x^2}{\rho_1}\frac{\partial}{\partial x}\left(\frac{w_{T,1}}{x^2}\right)\right] = 0 \tag{36}$$

$$w_{Y,1} = N_{Y,1}\frac{x^2}{a}\frac{\partial Y_1}{\partial x}, \qquad w_{T,1} = N_{T,1}\frac{x^2}{a}\frac{\partial T_1}{\partial x}$$

$$\frac{\partial \rho_1}{\partial t} + \frac{x}{a}\frac{\mathrm{d}a}{\mathrm{d}t}\frac{\partial \rho_1}{\partial x} - \frac{x^2}{a}\left[x^2\frac{\partial}{\partial x}\left(\frac{\rho_1 v_1}{x^2}\right)\right] = 0 \tag{37}$$

$$\frac{\partial v_1}{\partial t} - \frac{x^2}{a}\left[\left(v_1 - \frac{1}{x}\frac{\mathrm{d}a}{\mathrm{d}t}\right)\frac{\partial v_1}{\partial x} + \frac{1}{M\rho_1}\frac{\partial p_1}{\partial x}\right] = 0 \tag{38}$$

$$P_1 = \rho_1 R_1 T_1 \tag{39}$$

$$\frac{\partial Y_2}{\partial t} + \frac{1}{a-b}\left\{\left[v_2 - \frac{\mathrm{d}b}{\mathrm{d}t} - \left(\frac{\mathrm{d}a}{\mathrm{d}t} - \frac{\mathrm{d}b}{\mathrm{d}t}\right)x\right]\frac{\partial Y_2}{\partial x} + \frac{1}{\rho_2 r^2}\frac{\partial}{\partial x}(r^2 w_{Y,2})\right\} = 0 \tag{40}$$

$$\frac{\partial T_2}{\partial t} + \frac{1}{a-b}\left\{\left[v_2 - \frac{\mathrm{d}b}{\mathrm{d}t} - \left(\frac{\mathrm{d}a}{\mathrm{d}t} - \frac{\mathrm{d}b}{\mathrm{d}t}\right)x\right]\frac{\partial T_2}{\partial x} + \frac{1}{\rho_2 r^2}\frac{\partial}{\partial x}(r^2 w_{T,2})\right\} = 0 \tag{41}$$

$$w_{Y,2} = -N_{Y,2}\frac{1}{a-b}\frac{\partial Y_2}{\partial x}, \qquad w_{T,2} = -N_{T,2}\frac{1}{a-b}\frac{\partial T_2}{\partial x}$$

$$\frac{\partial \rho_2}{\partial t} - \frac{1}{a-b}\left[\frac{\mathrm{d}b}{\mathrm{d}t} + \left(\frac{\mathrm{d}a}{\mathrm{d}t} - \frac{\mathrm{d}b}{\mathrm{d}t}\right)x\right]\frac{\partial \rho^2}{\partial x} + \frac{1}{a-b}\frac{1}{r^2}\frac{\partial}{\partial x}(r^2\rho_2 v_2) = 0 \tag{42}$$

$$\frac{\partial v_2}{\partial t} + \frac{1}{a-b}\left\{\left[v_2 - \frac{\mathrm{d}b}{\mathrm{d}t} - \left(\frac{\mathrm{d}a}{\mathrm{d}t} - \frac{\mathrm{d}b}{\mathrm{d}t}\right)x\right]\frac{\partial v_2}{\partial x} + \frac{1}{M\rho_2}\frac{\partial p_2}{\partial x}\right\} = 0 \tag{43}$$

$$p_2 = \rho_2 R_2 T_2 \tag{44}$$

$$\frac{\partial T_3}{\partial t} - \frac{x}{b}\frac{db}{dt}\frac{\partial T_3}{\partial x} + \frac{1}{\rho_3 b x^2}\frac{\partial}{\partial x}(x^2 w_{T,3}) = 0 \tag{45}$$

$$w_{T,3} = -N_{T,3}\frac{1}{b}\frac{\partial T_3}{\partial x},$$

where Y_1 and Y_2 are the weight concentrations of oxygen and fuel vapor, respectively.

The boundary conditions at a large distance from the flame front are taken as

$$Y_1 = Y_\infty, \qquad T_1 = T_\infty, \qquad p_1 = p_\infty.$$

At the flame front, equations (9), (11), (19) and (20) give the following relations,

$$\left[\rho_1\left(v_1 - \frac{da}{dt}\right)\right]_{x=1} = \left[\rho_2\left(v_2 - \frac{da}{dt}\right)\right]_{x=1} \tag{46}$$

$$(p_1 - p_2)_{x=1} = M\left[\rho_1\left(v_1 - \frac{da}{dt}\right)(v_2 - v_1)\right]_{x=1} \tag{47}$$

$$\left(N_{Y,1}\frac{\partial Y_1}{\partial x}\right)_{x=1} = \gamma\frac{a}{a-b}\left(N_{Y,2}\frac{\partial Y_2}{\partial x}\right)_{x=1} \tag{48}$$

$$-h_c\left(N_{Y,2}\frac{\partial Y_2}{\partial x}\right)_{x=1} = \frac{a-b}{a}\left(\lambda_1\frac{\partial T_1}{\partial x}\right)_{x=1} + \left(\lambda_2\frac{\partial T_2}{\partial x}\right)_{x=1}, \tag{49}$$

and the assumption (ii) leads

$$(Y_1)_{x=1} = (Y_2)_{x=1} = 0. \tag{50}$$

For eleven quantities to be determined at the flame front, that is, Y_1, Y_2, T_1, T_2, ρ_1, ρ_2, p_1, p_2, v_1, v_2, and a, the number of the boundary conditions including the equation of state of the mixture at the front is eight. Equations (35)–(44) subjected to the boundary conditions at infinite are to define two quantities at the flame front, so that only one additional restriction is necessary to be imposed upon the quantities at the flame front. To this purpose, we assume (vii) the continuity of the temperature at the flame front, that is,

$$(T_1)_{x=1} = (T_2)_{x=1}. \tag{51}$$

The boundary conditions at the evaporating surface and the center of the droplet are given by the following equations in the same way as in 2.1;

$$\frac{db}{dt} = \frac{1}{\rho_3}\frac{1}{a-b}\left[\frac{N_{Y,2}}{1-Y_2}\frac{\partial Y_2}{\partial x}\right]_{x=0} \tag{52}$$

$$(u_2)_{x=0} = \left[1 - \frac{\rho_3}{\rho_2}\right]_{x=0}\frac{db}{dt} \tag{53}$$

$$h_l(\rho_2 v_2)_{x=0} = -\frac{1}{b}\left(\lambda_3\frac{\partial T_3}{\partial x}\right)_{x=1} + \frac{1}{a-b}\left(\lambda_2\frac{\partial T_2}{\partial x}\right)_{x=0} \tag{54}$$

$$(T_2)_{x=0} = (T_3)_{x=1} \tag{55}$$

$$(Y_2)_{x=0} = \exp\left[-\frac{h_l}{R_v T_s}\left(\frac{T_s}{T_2} - 1\right)_{x=0}\right] \tag{56}$$

$$\left(\frac{\partial T_3}{\partial x}\right)_{x=0} = 0. \tag{57}$$

For the initial conditions, we take a droplet of temperature T_l surrounded by the uniform mixture of temperature T_{b0}, pressure p_{b0} and fuel-vapor concentration Y_{b0} with a flame of temperature T_{a0} located at $r = a_0$ in a quiescent air at temperature T_∞, pressure p_∞ and oxygen concentration Y_∞, that is,

$$\begin{aligned}
&T_1 = T_\infty \quad p_1 = p_\infty \quad Y_1 = Y_\infty \quad v_1 = 0 && (r > a),\\
&T_a = T_{a0} \quad a = a_0 && (r = a),\\
&T_2 = T_{b0} \quad p_2 = p_\infty \quad Y_2 = Y_{b0} && \\
&\qquad\qquad v_2 = 0 && (a > r > b),\\
&T_b = T_l \quad b = 1 && (r = b),\\
&T_3 = T_l && (b > r).
\end{aligned} \tag{58}$$

The transformation of equations (35) to (58) into finite difference form with respect to space and time makes the quantities to be calculated

by stepwise Δt in time with a digital computer. The following figures represent the results of numerical calculations in this way, which display the processes of the combustions of benzene, methyl alcohol, ethyl alcohol, and *n*-octane in a still air at various temperatures, pressures and oxygen-concentrations. In the calculations, we used the physical properties of fuels and air shown in Table 1 and Fig. 2 with the same meshes of space and time as in the calculations of evaporation, 2.1.

The droplet has initially the temperature of 20°C and the radius of 1 mm. The other initial conditions concerning the flame temperature T_{a0}, the flame location a, the temperature of the mixture inside the flame T_{b0}, and the concentration of the fuel vapor Y_{b0} are not uniquely defined at the time of the initiation of combustion for such a front model. Conducting a preliminary computation in order to examine the effect of the arbitrariness of these initial values, we concluded that they would affect the process only in a few steps after the start of combustion, so that appropriate values for the initial conditions could be chosen without any change in the succeeding process of combustion except in a short time immediately after ignition.

Figure 8 shows the droplet-radius vs. time history of a burning droplet, which can be expressed in a linear function of time by the theory of quasi-steady model [4–6]. Figs. 8a, 8b, 8c and 8d represent the effects of the kind of fuel,

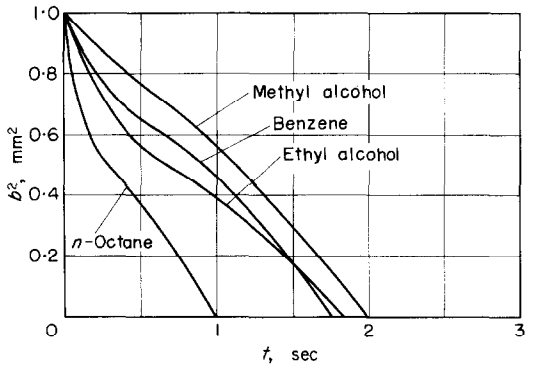

FIG. 8(a). Combustion of a droplet (effect of fuel, T_∞ = 300°C).

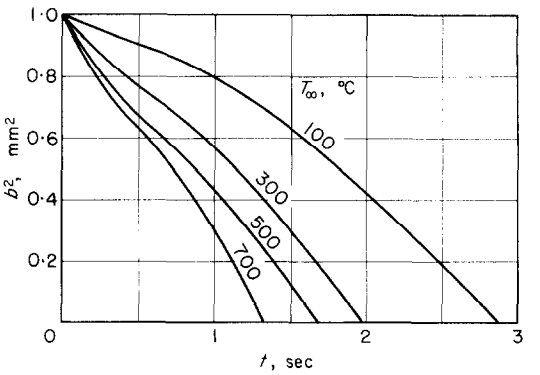

FIG. 8(b). Combustion of a droplet (effect of ambient temperature, methyl alcohol).

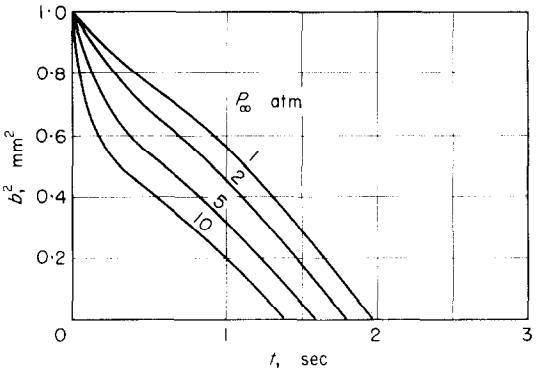

FIG. 8(c). Combustion of a droplet (effect of ambient pressure, methyl alcohol).

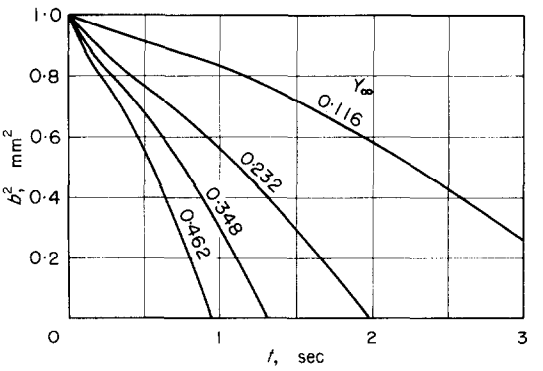

FIG. 8(d). Combustion of a droplet (effect of ambient oxygen-concentration, methyl alcohols).

the ambient temperature, the ambient pressure and the oxygen-concentration, respectively. The location of the flame front is shown in Fig. 9, the ratio of the flame radius to the droplet radius in Fig. 10, the surface temperature of the droplet in Fig. 11 and the temperature at the flame front in Fig. 12.

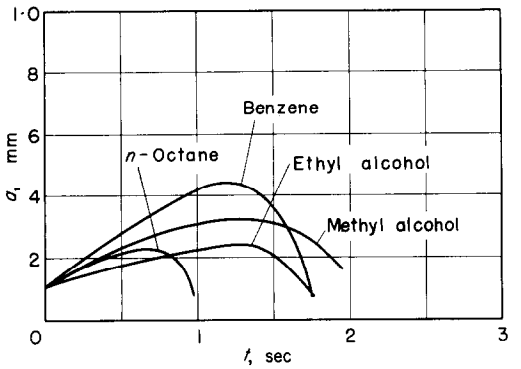

FIG. 9. Location of flame front ($T_\infty = 300°C$).

The burning coefficient defined as $|db^2/dt|$. which is constant in the quasi-steady model, being called as the burning constant, takes a large value in the initial period of combustion as shown in Fig. 8 and then approaches a constant value, which is nearly equal to the value obtained by the experimental works as well as to that of the quasi-steady model. The surface temperature of the droplet shown in Fig. 11 keeps nearly constant at first and then increases as the history curve in Fig. 8 becomes convex. These features with the comparison between the solid and the dotted curves in Figs. 3 and 4 suggest that the transfer processes of mass and heat would tend to be quasi-steady as the history curve of combustion becomes convex. The tendency to a quasi-steady state is also supported by the fact of the decreasing changes in the ratio of the flame radius to the droplet radius and in the flame temperature at such a time. The quasi-steady theory [6] for the combustion of a droplet in air at ambient

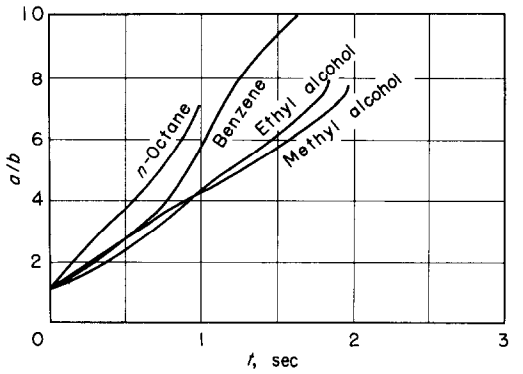

FIG. 10(a). Ratios of the flame radius to the droplet radius (effect of fuel, $T_\infty = 300°C$).

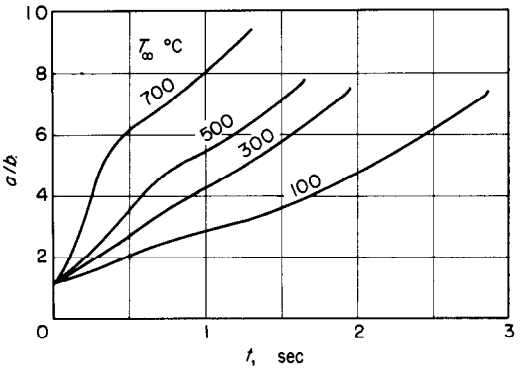

FIG. 10(b). Ratios of the flame radius to the droplet radius (effect of ambient temperature, methyl alcohol).

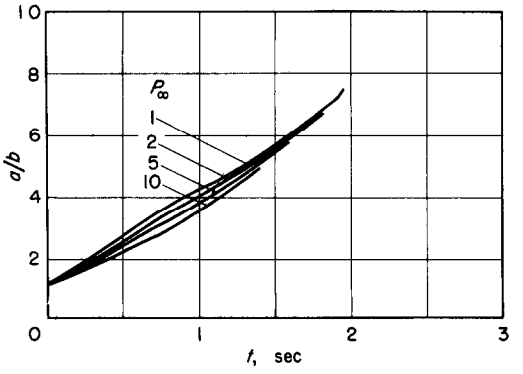

FIG. 10(c). Ratios of the flame radius to the droplet radius (effect of ambient pressure, methyl alcohol).

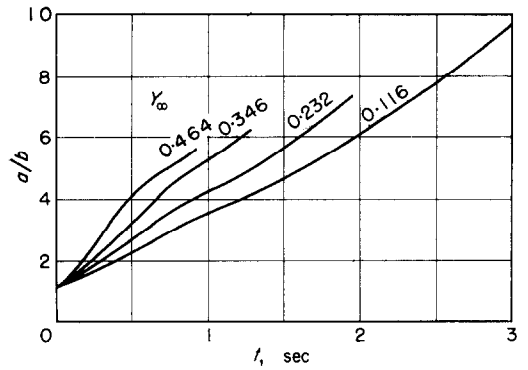

FIG. 10(d). Ratios of the flame radius to the droplet radius (effect of ambient oxygen-concentration, methyl alcohol).

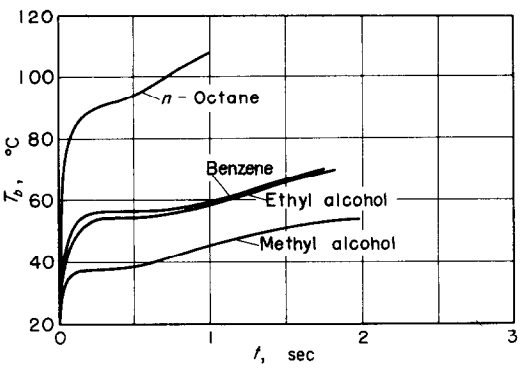

FIG. 11. Surface temperatures of burning droplets (T_∞ = 300°C).

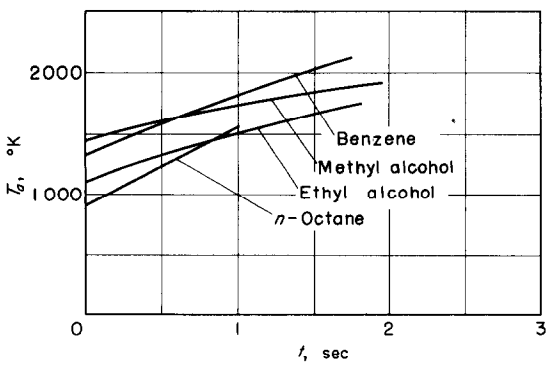

FIG. 12. Flame temperatures (T_∞ = 300°C).

temperature of 300°C predicts that for benzene the ratio of the flame radius to the droplet radius is 19·7 and the flame temperature is 2580°C and for ethyl alcohol they are 10·0 and 2400°C, respectively, which are considerably in excess of those shown in Figs. 10 and 12, though the compensation of the effects of the radius ratio and the flame temperature accounts for a satisfactory agreement of the burning rate between the values of the quasi-steady theory and the asymptotic values of the unsteady theory.

The increment in ambient temperatures makes the flame temperature increase by the same order in magnitude as shown in Figs. 8(b) and 10(b) to result in higher temperature at the droplet surface and higher burning coefficients. Since the dependence of the process on ambient pressures occurs through the changes in the boiling point and in the diffusivity coefficients, the effect of ambient pressures is distinguished upon the surface temperature of the droplet. On the contrary, the values of the radius ratio and the flame temperature are not so sensitive to ambient pressures. The oxygen concentration in ambient air affects directly the flame temperature and consequently the burning coefficient, but hardly excerts influence upon the radius ratio.

Figures 13–15 represent the space distributions of the temperature, the concentrations of fuel vapor and oxygen and the veloicity, respectively, when the droplet radius becomes half a value of the initial. The pressure distribution is always uniform in the limit of $\pm 10^{-4}p_\infty$ in time as well as in space.

In the above calculations, we used step distributions of the quantities in space at the initiation of combustion, as shown in equation (58). It should be noted that these initial distributions of the quantities, especially outside the flame front, could have a serious influence upon the results, though the distributions inside the flame are less influential. For example, if as the initial condition we take distributions of the quantities at a convex point in the $b^2 - t$ curve,

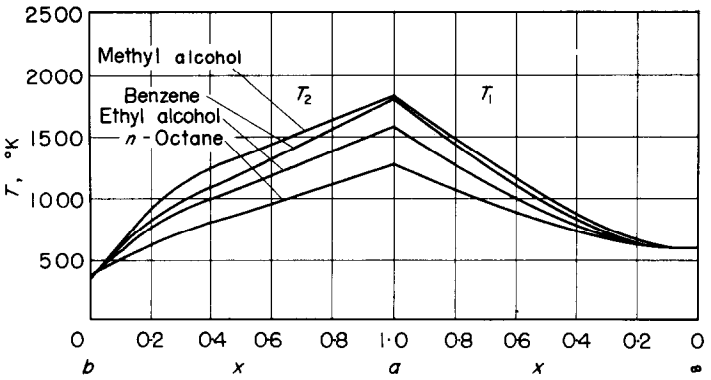

FIG. 13. Temperature distributions for combustion ($b = 0{\cdot}5$ mm, $T_\infty = 300°C$).

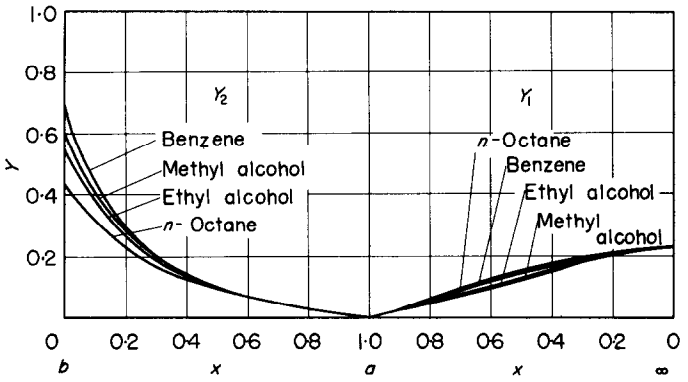

FIG. 14. Distributions of fuel-vapor concentration for combustions ($b = 0{\cdot}5$ mm, $T_\infty = 300°C$).

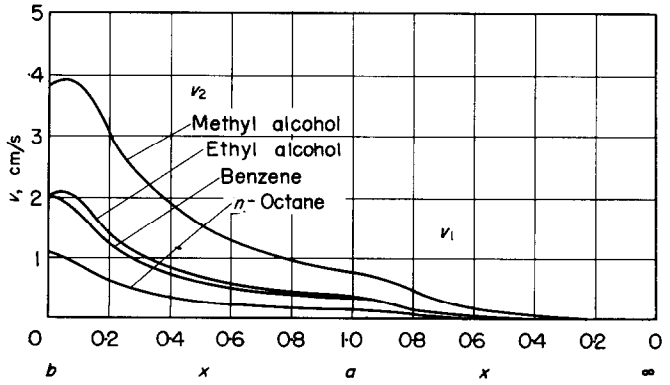

FIG. 15. Velocity distribution for combustion ($b = 0{\cdot}5$ mm, $T_\infty = 300°C$).

the recalculation with this initial condition results in a $b^2 - t$ curve which has no concave part. The same notice is valid in the case of evaporation treated in 2.1. It seems appropriate to remark finally that the dependence of the process on the initial distributions of quantities, which are not to be uniquely defined by the front model, requires some extension of the front model theory into the one in which the chemical kinetics of reaction can be taken into account in order to predict more completely the process of evaporation and combustion of a droplet.

3. CONCLUSION

The process of evaporation and combustion of a fuel droplet in a quiescent air is calculated numerically, treated as an unsteady diffusion-controlling phenomenon with the flame front model. Single droplets of liquid fuel—benzene, methyl alcohol, ethyl alcohol, and *n*-octane—are evaporated and burnt in air at various ambient temperatures and pressures and under various oxygen concentrations with the following results:

(1) The process of evaporation can not attain to a quasi-steady state of mass and heat transfer at the droplet surface,

(2) Concerning combustion, the process approaches at its end to a quasi-steady state, though the values of the flame temperature and the ratio of the flame radius to the droplet radius are much smaller than those of the quasi-steady model.

(3) The initial condition of the surrounding air of the droplet has an appreciable influence upon the process of evaporation and combustion.

REFERENCES

1. K. KOBAYASHI, On the evaporation rate of a liquid droplet in a hot gas, *J. Japan Soc. Mech. Engrs* 15–52, 14–19 (1949).
2. G. A. E. GODSAVE, Studies of the combustion of drops in a fuel spray, *4th International Symposium on Combustion*, pp. 818–830. Williams & Wilkins, Baltimore (1953).
3. D. B. SPALDING, The combustion of liquid fuel, *4th International Symposium on Combustion*, pp. 847–864. Williams & Wilkins, Baltimore (1953).
4. M. GOLDSMITH and S. S. PENNER, On the burning of single drops of fuel in a oxidizing atmosphere, *Jet Propulsion* **24**, 245–251 (1954).
5. H. WISE, J. LORELL and J. WOOD, The effects of chemical and physical parameters on the burning rate of a liquid droplet, *5th International Symposium on Combustion*, pp. 132–141. Reinhold, New York (1954).
6. T. OZAKI and M. GOMI, The combustion and evaporation of a fuel droplet, *J. Japan Soc. Mech. Engrs* 19–88, 1–6 (1953).
7. K. KOBAYASHI, A study on the evaporation and combustion of a single droplet, *J. Japan Soc. Mech. Engrs* 20–100, 826–843 (1954).
8. M. GOLDSMITH, Experiments on the burning of single droplets of fuel, *Jet Propulsion* **26**, 172–168 (1956).
9. E. G. MASDIN and M. W. THRING, Combustion of single droplets of liquid fuel, *J. Inst. Fuel* **41**, 251–260 (1962).
10. H. ISODA and S. KUMAGAI, New aspects of droplet combustion, *7th International Symposium on Combustion*, pp. 523–531. Butterworths, London (1958).

Résumé—Le processus d'évaporation et de combustion d'une gouttelette liquide dans de l'air au repos est calculé numériquement, en le traitant comme un phénomène instationnaire contrôlé par la diffusion avec la flamme à partir du modèle. Des gouttelettes uniques de combustible liquide-benzène, alcool méthylique, alcool éthylique, n-octane-sont évaporées et brulées dans l'air sous différentes températures ambiantes, pressions et concentrations en oxygène. Le processus d'évaporation ne peut pas parvenir à un état quasi-permanent de transport de masse et de chaleur à la surface de la gouttelette. Concernant la combustion, le processus tend asymptotiquement vers un état quasi-permanent, bien que les valeurs de la température de la flamme et le rapport du rayon de la goutte soient beaucoup plus faibles que ceux de la théorie quasi-permanente. La condition initiale de l'air environnant a une grande influence sur les processus d'évaporation et de combustion.

Zusammenfassung—Der Prozess der Verdampfung und Verbrennung eines Flüssigkeitströpfchens in ruhender Luft wurd numerisch berechnet. Das Problem wird dabei als instationäres Phänomen betrachtet und mit Hilfe des Flammenfront-Modells behandelt. Einzelne Tröpfchen von flüssigem Brennstoff -Benzol, Methylalkohol, Äthylalkohol, n-Oktanwurden bei verschiedenen Umgebungstemperaturen, Drücken

und Sauerstoff-Konzentrationen verdampft und verbrannt. Der bei der Verdampfung auftretende Stoff- und Wärmeübergang an der Tröpfchenoberfläche wird nicht quasistationär. Hingegen wird die Verbrennung am Ende quasistationär, obwohl die Werte der Flammentemperatur und des Verhältnisses Flammenradius zu Tröpfchenradius viel kleiner sind als diejenigen, die der quasistationären Theorie entsprechen. Der Anfangszustand der umgebenden Luft hat einen grossen Einfluss auf den Prozess der Verdampfung und Verbrennung.

Аннотация—Процесс испарения и горения капельки жидкости в спокойном воздухе рассчитывается численно и рассматривается как нестационарное контролируемое диффузией явление с помощью модели фронта пламени. Единичные капельки жидкого топлива-бензина, метилового спирта, этилового спирта, *n* — октана — испаряются и сгорают в воздухе при различных температурах и давлениях окружающей среды и концентрациях кислорода. В процессе испарения не может быть достигнуто квазистационарное состояние переноса массы и тепла у поверхности капельки. Что касается горения, то процесс в конце приближается к квазистационарному состоянию, хотя значения температуры пламени и отношение радиуса пламени к радиусу капельки значительно меньше, чем по квазистационарной теории. Начальное состояние окружающего воздуха оказывает большое влияние на процесс испарения и горения.